Drug Delivery

International Edition: DOI: 10.1002/anie.201501748
German Edition: DOI: 10.1002/ange.201501748

Mussel-Inspired Protein Nanoparticles Containing Iron(III)–DOPA Complexes for pH-Responsive Drug Delivery**

*Bum Jin Kim, Hogyun Cheong, Byeong Hee Hwang, and Hyung Joon Cha**

Abstract: *A novel bioinspired strategy for protein nanoparticle (NP) synthesis to achieve pH-responsive drug release exploits the pH-dependent changes in the coordination stoichiometry of iron(III)–3,4-dihydroxyphenylalanine (DOPA) complexes, which play a major cross-linking role in mussel byssal threads. Doxorubicin-loaded polymeric NPs that are based on Fe^{III}–DOPA complexation were thus synthesized with a DOPA-modified recombinant mussel adhesive protein through a co-electrospraying process. The release of doxorubicin was found to be predominantly governed by a change in the structure of the Fe^{III}–DOPA complexes induced by an acidic pH value. It was also demonstrated that the fabricated NPs exhibited effective cytotoxicity towards cancer cells through efficient cellular uptake and cytosolic release. Therefore, it is anticipated that Fe^{III}–DOPA complexation can be successfully utilized as a new design principle for pH-responsive NPs for diverse controlled drug-delivery applications.*

In recent decades, nanoparticles (NPs) with multiple functionalities, such as sustained release, molecular targeting, and environmental responsiveness, have been developed.[1] In particular, responsive behaviors against various types of physical and chemical signals have been introduced into NPs as a design strategy for causing them to release drugs when exposed to particular external stimuli.[2] Among several possible environmental stimuli, the pH value has been widely exploited as an important chemical cue for the design of responsive NPs.[3] The most widely applicable target of such pH-responsive NPs at the cellular level is the intracellular delivery of anti-cancer drugs through acidified endosomal compartments, where the pH value rapidly drops below 6.[4] As overcoming endosomal acidification has come to be regarded as a major hurdle for the highly concentrated delivery of many types of anti-cancer drugs to the cytosol of cancer cells,[2a,5] the ability of NPs to deliver drugs in a pH-responsive fashion may be a considerable advantage for applications in cancer therapy.

In the proteinaceous cuticles that cover mussel byssal threads, metal catechol coordination complexes between Fe^{III} and 3,4-dihydroxyphenylalanine (DOPA) were discovered, and these complexes were found to serve as key cross-linking mediators for the material's outstanding mechanical properties.[6] Moreover, the binding in these Fe^{III}–DOPA complexes is known to be reversible and nearly as strong as covalent bonds, and the stoichiometry of the bidentate ligand/metal binding can be altered by the environmental pH value to form one, two, or three Fe^{III}–DOPA cross-links.[7] Using these characteristics, many researchers developed mussel-inspired biomaterials containing Fe^{III}–DOPA complexes with high mechanical performance and self-healing properties for biomedical applications.[8]

In particular, Fe^{III}–DOPA complexes have been applied in the field of NPs. However, most previous studies have focused on exploiting Fe^{III}–DOPA complexes for the surface modification of metal oxide NPs, introducing stabilizing polymers such as poly(ethylene glycol) and altering the magnetic properties of iron oxide NPs.[9] However, to the best of our knowledge, the pH-responsive properties of the Fe^{III}–DOPA complexes themselves have never been directly exploited for controlled drug delivery.

Herein, we report a novel strategy for the synthesis of polymeric NPs that is based on mussel adhesive proteins (MAPs) to achieve pH-induced drug release by changes in the pH-responsive Fe^{III}–DOPA coordination stoichiometry (Scheme 1). We exploited recombinantly produced DOPA-containing MAPs, which have been introduced in previous studies,[10] to fabricate protein NPs through a co-electrospraying process with an anti-cancer drug. As a proof of concept, we successfully demonstrated that these MAP-based Fe^{III}–DOPA NPs exhibited pH-responsive drug-release profiles and cytotoxic effects on cancer cells by effective cellular uptake and cytosolic release in vitro.

To synthesize NPs that contain Fe^{III}–DOPA complexes, we employed twelve tandem-repeat decapeptides (AKPSYPPTYK) of *Mytilus* mussel foot protein type 1 (fp-1). This protein can be successfully produced using a recombinant bacterial expression system with DOPA residues in the position of the tyrosine residues according to an in vitro enzymatic modification procedure using mushroom tyrosinase, as previously reported.[8c,d] By amino acid composition analysis, we found that approximately 7 mol% of DOPA (ca. 30% of the total tyrosine residues) had been introduced into the recombinant fp-1 proteins (Supporting Information, Figure S1).

[*] Dr. B. J. Kim, H. Cheong, Dr. B. H. Hwang, Prof. H. J. Cha
Department of Chemical Engineering
Pohang University of Science and Technology
Pohang 790-784 (Korea)
E-mail: hjcha@postech.ac.kr
Dr. B. H. Hwang
Division of Bioengineering
Incheon National University
Incheon 406-772 (Korea)

[**] Financial support was provided by the Marine Biotechnology Program (Marine BioMaterials Research Center) funded by the Ministry of Oceans and Fisheries, Korea. DOPA = 3,4-dihydroxyphenylalanine.

Supporting information for this article is available on the WWW under http://dx.doi.org/10.1002/anie.201501748.

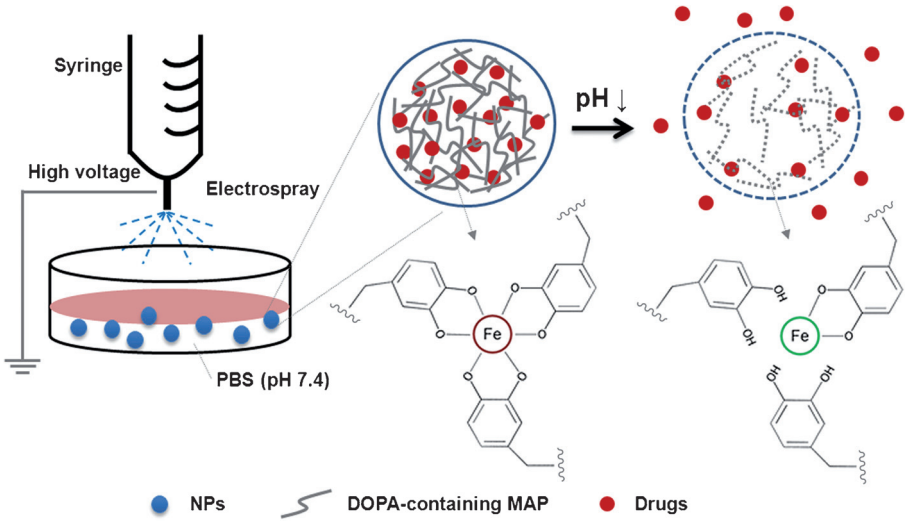

Scheme 1. Synthesis of polymeric NPs based on Fe^{III}–DOPA complexation with recombinant DOPA-containing MAP using an electrospraying process to achieve pH-responsive drug release.

Electrospraying has been found to be one of the most efficient methods of preparing polymeric NPs for drug-delivery systems because of its ability to produce particles of a small and uniform size, its rapid and simple procedures, its high reproducibility and scale-up productivity, and its effective drug-encapsulation capability.[11] Many types of commonly used synthetic and natural biopolymers have been used for this purpose, and many types of drugs have also been loaded into electrosprayed polymeric NPs through co-electrospraying and coaxial electrospraying methods.[12] Therefore, we applied the electrospraying method to synthesize NPs based on the DOPA-modified recombinant fp-1 (*m*fp-1) proteins. As the electrospraying of an *m*fp-1 solution had previously never been attempted, we first optimized several processing conditions. A water-based solvent was chosen instead of an organic solvent to exclude the possibly toxic effect of any remaining solvent after the electrospraying process; we ultimately used distilled water with 70% ethanol to enhance the degree of evaporation. We considered that the protein concentration and the applied voltage might be key factors in the optimization. After electrospraying *m*fp-1 onto aluminum foil, we found that a high voltage of 6–14 kV, suitable for the stable ejection of the protein solution, was required for the preparation of the NPs, and an *m*fp-1 protein concentration of 1.5% seemed to be optimal because a fibrous structure began to appear at concentrations of greater than 3% (Figure 1a and Figure S2).

In fact, we found that the electrosprayed *m*fp-1 NPs that were prepared in this manner were not suitable for further analysis because of a loss in particle morphology that occurred upon dissolution in aqueous solution. We surmised that the introduction of Fe^{III}–DOPA complexes into the *m*fp-1 NPs might not only prevent them from dissolving, but also render them pH-responsive. Therefore, we induced the formation of tris-coordinated Fe^{III}–DOPA cross-links by adding Fe^{III} ions into the *m*fp-1 solution to achieve a molar ratio of Fe^{III}/DOPA = 1:3 before the electrospraying process. The formation of the desired complexes was confirmed by an immediate color change to purple.[8c] Afterwards, we attained simultaneous Fe^{III}–DOPA cross-links within the *m*fp-1 nanoparticles by electrospraying the complexes directly into a buffer solution of pH 7.4. We also observed that the color of the electrosprayed solution became slightly pink, indicating the presence of Fe^{III} complexes with two or three DOPA ligands, which were spectroscopically identified by UV/Vis spectrophotometric analysis (data not shown). Typical absorbance peaks near 500 nm (pink) and 560 nm (purple) indicated the formation of Fe^{III} complexes with two or three DOPA ligands, respectively.[13]

Next, drug loading into the *m*fp-1 NPs that contained the

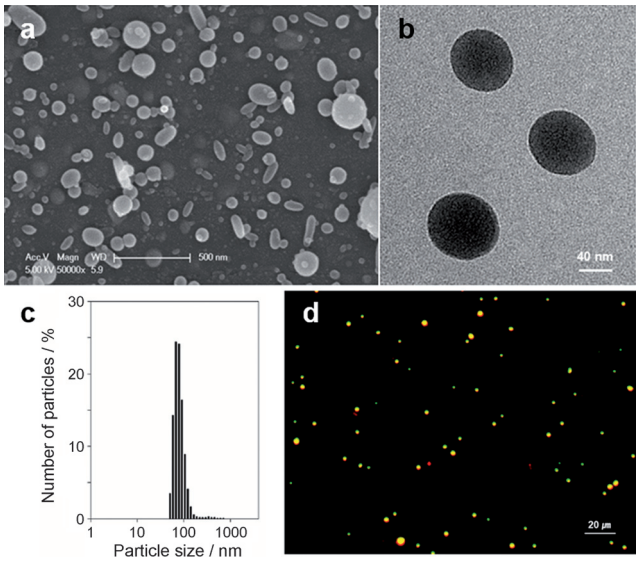

Figure 1. a) Scanning electron microscopy (SEM) and b) transmission electron microscopy (TEM) morphological characterizations of the electrosprayed DOX-loaded *m*fp-1 NPs. c) Particle size distribution of the DOX-loaded *m*fp-1 NPs as determined by DLS. d) Merged fluorescence microscopy images of electrosprayed DOX-loaded FITC-conjugated fp-1 NPs.

Fe^{III}–DOPA complexes was attempted using the co-electrospraying process. The co-electrospraying process is a method of generating nanoparticulate droplets using simple mixed solutions of polymers and drugs. Doxorubicin (DOX) was used as a model drug in our study. DOX is one of the most widely used commercial anti-breast-cancer drugs, but controlled drug-delivery approaches using polymeric nanoconjugates are required because of its cytotoxicity to normal tissues and the induction of acute cardiotoxicity.[14] In our experiments, DOX-loaded *m*fp-1 NPs were successfully synthesized by co-electrospraying a mixture of DOX and *m*fp-1 solutions that contained Fe^{III}–DOPA complexes. Through direct elec-

trospraying, the DOX-loaded NPs were dispersed in a physiological buffer solution after the unloaded DOX molecules were removed from the same solution through dialysis. Electron microscopy analyses revealed that the morphology of the DOX-loaded *m*fp-1 NPs was spherical (Figure 1a, b), and the DOX-loaded *m*fp-1 NPs were determined to be approximately 80–130 nm in size by dynamic light scattering (DLS) measurements (Figure 1c). The drug loading efficiency was calculated to be approximately 50–75% (Table S1), and we found that the loading efficiency could be altered by modifying the molar mixing ratio between *m*fp-1 and DOX. Considering the amounts of unloaded DOX that was obtained during electrospraying, DOX-loaded *m*fp-1 NPs that were synthesized using a 1:1 molar ratio of *m*fp-1/DOX were selected for all further studies. Using the fluorescence detection characteristics of DOX and fluorescein isothiocyanate (FITC) conjugated fp-1, we clearly observed the co-localization of the NPs and DOX by fluorescence microscopy (Figure 1d and Figure S3).

To evaluate whether these DOX-loaded *m*fp-1 NPs had the ability to release DOX in a pH-responsive manner, we investigated the in vitro DOX release profiles by monitoring the released DOX passing through a dialysis membrane as a function of incubation time in different pH environments. We observed significantly increased DOX release in a pH 6 buffer compared with other buffers of higher pH values (Figure 2a), thus indicating that DOX release is indeed pH-dependent. Furthermore, the approximately four-fold enhancement in DOX release under acidic conditions that was detected during the first three hours of incubation accentuates the pH-responsive release behavior of the *m*fp-1 NPs. Furthermore, we observed a gradual disappearance of the initial purple/pink color as well as a decrease in the spectroscopic absorptions at approximately 500 and 540 nm upon incubation in more acidic buffers (Figure S4), indicating that the number of coordination bonds between Fe^{III} and DOPA was gradually reduced. These results are in good agreement with the results of our previous studies regarding hydrogel and nanofiber systems based on Fe^{III}–DOPA complexation.[8c,d]

The induction of drug release using pH-labile cross-linkers is one of the most effective strategies for pH-dependent release systems. Many types of conjugation reactions that feature various cleavage sites have been utilized by means of pH-accelerated hydrolysis to synthesize polymeric NPs.[3a] Consistent with these studies, our drug-release system that is based on pH-dependent Fe^{III}–DOPA complexes may also rely on a similar mechanism, that is, drugs in tightly packed polymers may be able to diffuse through the pH-induced loosening of the cross-linked networks. Importantly, the enhanced drug-release properties in acidic conditions clearly support the hypothesis that the *m*fp-1 NPs containing Fe^{III}–DOPA complexes act in a pH-responsive way.

To confirm the cytotoxic effects of the DOX-loaded *m*fp-1 NPs on cancer cells, we examined the cell viabilities before and after simple treatments involving the introduction of the original *m*fp-1 NPs, DOX-loaded *m*fp-1 NPs, and free DOX into the culture media using the HeLa cell line, which is known to be derived from cervical cancer tissues. At certain concentrations (1–10 $\mu g\,mL^{-1}$), DOX has been reported to reduce the cell viabilities of several cell lines, including in HeLa cells.[15] We found that the original *m*fp-1 NPs without DOX had no cytotoxic effect on the cells (Figure 2b). However, the *m*fp-1 NPs that contained DOX exhibited significant cytotoxicity against the cancer cells, and the half-maximal inhibitory concentration (IC_{50}) value was determined to be approximately 2 $\mu g\,mL^{-1}$. This value is twice as high as that of free DOX (ca. 1 $\mu g\,mL^{-1}$), which served as a positive control (Figure 2b). The relatively high sensitivity of the cell viability towards free DOX is reasonable because of the characteristics of free DOX, which can easily permeate into the cytosol without encountering any endosomal barrier. Importantly, given the effective cytotoxicity of the DOX-loaded *m*fp-1 NPs, we confirmed that the acidic environment of the endosomes actually promotes the release of DOX inside the *m*fp-1 NPs into the cytosol.

Fluorescence microscopy images that show the cellular uptake behavior of DOX-loaded *m*fp-1 NPs support the hypothesis that the release of DOX into the cytosol is a major factor contributing to the cytotoxic effect of these NPs towards the cancer cells (Figure 3). We clearly observed that one hour after treatment, the DOX was localized near the cell membrane, and it took approximately three hours for the DOX to spread through the cytosol, including to the cell nucleus (Figure 3a). In contrast, we could detect the spread of DOX throughout the entire cell area after treatment with free DOX for one hour (Figure S5). We also measured the DOX uptake at the single-cell level by fluorescence detection using flow cytometry. In consistency with the imaging analysis results, a strong fluorescence signal was measured for the cells treated with DOX-loaded *m*fp-1 NPs, and the intensity gradually increased with increasing incubation time (Figure 3b). The intensity of the fluorescence was higher in cells treated with free

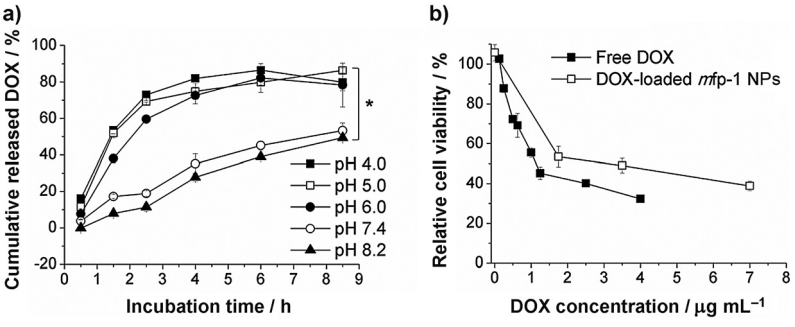

Figure 2. a) In vitro DOX release profiles of the DOX-loaded *m*fp-1 NPs at different pH values. Values and error bars represent the means of triplicate samples and standard deviations with statistical significance (* $p < 0.05$). b) Relative HeLa cell viability with DOX-loaded *m*fp-1 NPs at different DOX concentrations. A DOX concentration of zero corresponds to the cell viability after treatment with the original *m*fp-1 NPs without DOX. Values and error bars represent the means of triplicate samples and standard deviations.

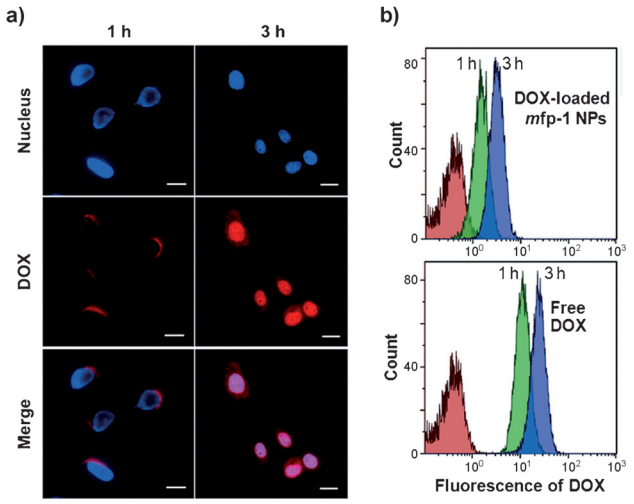

Figure 3. a) Fluorescence microscopy images and b) flow cytometry analysis of HeLa cells incubated with DOX-loaded *m*fp-1 NPs for one and three hours. A concentration of 2 $\mu g\,mL^{-1}$ was used for both the DOX-loaded *m*fp-1 NPs and free DOX. Cell nuclei were stained with Hoechst 33258 (blue). Scale bar: 20 μm.

DOX than in cells treated with DOX-loaded *m*fp-1 NPs. Typically, with the exception of extremely small NPs (< 50 nm), NPs that are smaller than 500 nm are believed to be internalized into cells through endocytosis, which is known to be a highly energy-dependent process that is mediated by diverse molecular factors.[16] Several of our results, such as the retarded cellular uptake relative to that of free DOX, the pH-responsive release properties, and the appropriate particle size (80–100 nm) of the DOX-loaded *m*fp-1 NPs, collectively suggest that an endocytosis process followed by endosomal escape may be the mechanism through which the *m*fp-1 NPs induce cytosolic DOX release and the resulting cytotoxicity.

The preparation of novel *m*fp-1 NPs and the achievement of pH-responsive drug release by Fe^{III}–DOPA complexation in this study not only raise several scientific questions and provide some corresponding answers but also offer the opportunity to proceed with further research towards potential future applications. First, even though we have suggested that the intracellular delivery of *m*fp-1 NPs may occur through an endocytosis process, a more precise study of the mechanism is necessary. To that end, an investigation of the possible endosomal escape processes of *m*fp-1 itself would be a good starting point because of several pieces of evidence, including the "proton sponge effect" of NPs based on various types of basic polymers (e.g., histone, polyethylenimine, and chitosan)[17] as well as the previously reported gene-delivery function of MAP and DNA polyplexes.[18] Second, it is expected that Fe^{III}–DOPA complexes could be readily applied to other polymer systems to achieve pH-responsive drug delivery because there have been many studies that employed catechol groups as pendants on diverse polymer backbones by chemical conjugation strategies.[8b,19] In combination with these efforts, our new delivery strategy using Fe^{III}–DOPA complexation can become a versatile chemical method for pH-responsive drug release for many other biomaterials. Lastly, it may be possible to utilize our adhesive-protein-based NPs as local drug-delivery agents by exploiting the adhesion properties on wet tissue surfaces (Figure S6), which may significantly reduce diffusive losses of the locally injected NPs. Furthermore, our *m*fp-1 NPs based on Fe^{III}–DOPA complexation could be candidates for systematic cancer therapy and gene-delivery applications. However, a stricter regulation of the drug release that occurs under physiological conditions would be required, and efforts to increase the stability of these NPs in body fluid for efficient delivery in actual tissues should be pursued.

In summary, novel drug-loaded NPs based on mussel-derived adhesive proteins were fabricated in a co-electrospraying process, and the formation of stable cross-links and pH-responsive drug release were achieved in these NPs by stoichiometric Fe^{III}–DOPA complexation. We found that NPs containing Fe^{III}–DOPA complexes have a cytotoxic effect on a cancer cell line as a result of efficient cellular uptake and cytosolic release. We strongly anticipate that these MAP-based Fe^{III}–DOPA NPs could be useful as delivery platforms for drug and gene therapies.

Keywords: drug delivery · electrospray · iron complexes · nanoparticles · proteins

How to cite: *Angew. Chem. Int. Ed.* **2015**, *54*, 7318–7322
Angew. Chem. **2015**, *127*, 7426–7430

[1] a) O. C. Farokhzad, R. Langer, *ACS Nano* **2009**, *3*, 16–20; b) L. Zhang, F. X. Gu, J. M. Chan, A. Z. Wang, R. S. Langer, O. C. Farokhzad, *Clin. Pharmacol. Ther.* **2008**, *83*, 761–769.
[2] a) M. Elsabahy, K. L. Wooley, *Chem. Soc. Rev.* **2012**, *41*, 2545–2561; b) M. S. Muthu, C. V. Rajesh, A. Mishra, S. Singh, *Nanomedicine* **2009**, *4*, 657–667.
[3] a) W. Gao, J. M. Chan, O. C. Farokhzad, *Mol. Pharm.* **2010**, *7*, 1913–1920; b) S. Manchun, C. R. Dass, P. Sriamornsak, *Life Sci.* **2012**, *90*, 381–387.
[4] K. A. Whitehead, R. Langer, D. G. Anderson, *Nat. Rev. Drug Discovery* **2009**, *8*, 129–138.
[5] a) J. K. Vasir, V. Labhasetwar, *Adv. Drug Delivery Rev.* **2007**, *59*, 718–728; b) M. J. Marín, F. Galindo, P. Thomas, D. A. Russell, *Angew. Chem. Int. Ed.* **2012**, *51*, 9657–9661; *Angew. Chem.* **2012**, *124*, 9795–9799.
[6] a) Z. Xu, *Sci. Rep.* **2013**, *3*, 2914; b) M. J. Harrington, A. Masic, N. Holten-Andersen, J. H. Waite, P. Fratzl, *Science* **2010**, *328*, 216–220.
[7] H. Zeng, D. S. Hwang, J. N. Israelachvili, J. H. Waite, *Proc. Natl. Acad. Sci. USA* **2010**, *107*, 12850–12853.
[8] a) B. P. Lee, P. B. Messersmith, J. N. Israelachvili, J. H. Waite, *Annu. Rev. Mater. Res.* **2011**, *41*, 99–132; b) N. Holten-Andersen, M. J. Harrington, H. Birkedal, B. P. Lee, P. B. Messersmith, K. Y. Lee, J. H. Waite, *Proc. Natl. Acad. Sci. USA* **2011**, *108*, 2651–2655; c) B. J. Kim, S. Kim, D. X. Oh, A. Masic, H. J. Cha, D. S. Hwang, *J. Mater. Chem. B* **2015**, *3*, 112–118; d) B. J. Kim, D. X. Oh, S. Kim, J. H. Seo, D. S. Hwang, A. Masic, D. K. Han, H. J. Cha, *Biomacromolecules* **2014**, *15*, 1579–1585; e) M. Krogsgaard, M. A. Behrens, J. S. Pedersen, H. Birkedal, *Biomacromolecules* **2013**, *14*, 297–301.
[9] a) A. K. Yuen, G. A. Hutton, A. F. Masters, T. Maschmeyer, *Dalton Trans.* **2012**, *41*, 2545–2559; b) H. J. Lee, A. N. Koo, S. W. Lee, M. H. Lee, S. C. Lee, *J. Controlled Release* **2013**, *170*, 198–208.
[10] a) H. J. Cha, D. S. Hwang, S. Lim, *Biotechnol. J.* **2008**, *3*, 631–638; b) D. S. Hwang, Y. Gim, H. J. Yoo, H. J. Cha, *Biomaterials* **2007**, *28*, 3560–3568.

[11] R. Sridhar, S. Ramakrishna, *Biomatter.* **2013**, *3*, 24281 – 24292.
[12] a) M. Gulfam, J. E. Kim, J. M. Lee, B. Ku, B. H. Chung, B. G. Chung, *Langmuir* **2012**, *28*, 8216 – 8223; b) Y. Wu, B. Yu, A. Jackson, W. Zha, L. J. Lee, B. E. Wyslouzil, *Mol. Pharm.* **2009**, *6*, 1371 – 1379; c) J. Lahann, *Small* **2011**, *7*, 1149 – 1156.
[13] S. W. Taylor, D. B. Chase, M. H. Emptage, M. J. Nelson, J. H. Waite, *Inorg. Chem.* **1996**, *35*, 7572 – 7577.
[14] a) M. Khasraw, R. Bell, C. Dang, *Breast J.* **2012**, *21*, 142 – 149; b) S. Vijayaraghavalu, J. K. Dermawan, V. Cheriyath, V. Labhasetwar, *Mol. Pharm.* **2013**, *10*, 337 – 352.
[15] a) B. Yang, Y. Lv, J. Y. Zhu, Y. T. Han, H. Z. Jia, W. H. Chen, J. Feng, X. Z. Zhang, R. X. Zhuo, *Acta Biomater.* **2014**, *10*, 3686 – 3695; b) L. Qiu, M. Qiao, Q. Chen, C. Tian, M. Long, M. Wang, Z. Li, W. Hu, G. Li, L. Cheng, L. Cheng, H. Hu, X. Zhao, D. Chen, *Biomaterials* **2014**, *35*, 9877 – 9887.
[16] a) V. P. Torchilin, *Adv. Drug Delivery Rev.* **2006**, *58*, 1532 – 1555; b) K. Y. Win, S.-S. Feng, *Biomaterials* **2005**, *26*, 2713 – 2722.
[17] a) H. Storrie, D. J. Mooney, *Adv. Drug Delivery Rev.* **2006**, *58*, 500 – 514; b) G. Creusat, A. S. Rinaldi, E. Weiss, R. Elbaghdadi, J. S. Remy, R. Mulherkar, G. Zuber, *Bioconjugate Chem.* **2010**, *21*, 994 – 1002.
[18] D. S. Hwang, K. R. Kim, S. Lim, Y. S. Choi, H. J. Cha, *Biotechnol. Bioeng.* **2009**, *102*, 616 – 623.
[19] a) D. G. Barrett, D. E. Fullenkamp, L. He, N. Holten-Andersen, K. Y. C. Lee, P. B. Messersmith, *Adv. Funct. Mater.* **2013**, *23*, 1111 – 1119; b) H. Ceylan, M. Urel, T. S. Erkal, A. B. Tekinay, A. Dana, M. O. Guler, *Adv. Funct. Mater.* **2013**, *23*, 2081 – 2090.

Received: February 27, 2015
Revised: April 4, 2015
Published online: May 12, 2015

